



The reduction of chromite ore processing residues by green tea synthesized nano zerovalent iron and its solidification/stabilization in composite geopolymer

Faheem Muhammad^{a, b}, Ming Xia^a, Shan Li^a, Xu Yu^a, Yanhong Mao^a,
Farooq Muhammad^c, Xiao Huang^{a, b, *}, Binquan Jiao^{a, b, *}, Lin Yu^{a, b, *}, Dongwei Li^{a, b, *}

^a State Key Laboratory for Coal Mine Disaster Dynamics and Control, Chongqing University, Chongqing, 400044, PR China

^b College of Resource and Environmental Science, Chongqing University, Chongqing, 400044, China

^c Key Laboratory of Three Gorges Reservoir Region's Eco Environment Ministry of Education, School of Urban Construction and Environmental Engineering, Chongqing University, Chongqing, 400045, PR China

ARTICLE INFO

Article history:

Received 25 March 2019

Received in revised form

5 May 2019

Accepted 1 June 2019

Available online 21 June 2019

Handling Editor: Panos Seferlis

Keywords:

Green synthesis

Zerovalent iron nanoparticles

Chromite ore processing residues

Geopolymer

Solidification/stabilization

ABSTRACT

The present study is aimed to reduce the environmental footprints resulted from chromite ore processing residues (COPR); a hazardous waste having Cr(VI). The solidification/stabilization of COPR through geopolymer coupled with green tea synthesized nano zerovalent iron (GT-NZVI) is an effective approach to deal with this challenge. Therefore, the blast furnace slag and metakaolin were used to prepare the composite based geopolymer and GT-NZVI particles were synthesized by oolong tea in current experiment. The GT-NZVI treated and untreated COPR was solidified in composite geopolymer. The efficiency of solidified products was evaluated through compressive strength and leaching analysis. The results depicted that varying sizes of GT-NZVI particles were successively synthesized which could be utilized for reduction of Cr(VI) existed in COPR. The solidified products having GT-NZVI treated COPR (GCM (GT-NZVI) and untreated COPR (GCM) had compressive strength of 33Mpa and 47 MPa, respectively up to 50% addition of COPR waste. The immobilization effect of GCM (GT-NZVI) samples were better than GCM samples. The leaching toxicity of Cr(VI) in both GCM (GT-NZVI) and GCM samples was far below than safe limits (<5 mg/L). In addition, the fourier transform infrared spectrometry, X-Ray diffraction, scanning electron microscope equipped with energy dispersive spectrometer analysis had verified that COPR was effectively solidified in composite based geopolymer by physical and chemical means.

© 2019 Published by Elsevier Ltd.

1. Introduction

In start of 19th century, the chromium salt production has gained popularity in industrial sectors due to its use in leather tanning, stainless steel production, metallurgy, dyestuff, pigment, metal polishing, wood preservative etc. (Lehoux et al., 2017). Basically, the chromium salt is produced by two ways which includes high lime and non-lime process. High lime process is considered as outdated because each ton of Cr produces 2–3 t of hazardous solid waste called chromium ore processing residues (COPR). The COPR is a hazardous waste due to presence of hexavalent chromium/Cr(VI)

which is highly mobile and carcinogenic in nature. Therefore, COPR production through high lime process is prohibited in UK and USA. While, Pakistan, China, India and Russia are still using high lime process and facing the problems associated with COPR (Yu et al., 2012). The COPR associated problems are; (a) high utilization of lands during its storage as heaps and (b) increase in leaching concentration results in contamination of ecosystem (Dermatas et al., 2006). Hence, resourceful utilization/remediation of COPR is necessary which can prevent the leaching and contamination of Cr(VI).

Generally, Cr(VI) remediation technologies are classified into three broad categories i.e. toxicity reduction, removal and contaminants. More specifically, the researchers had remediated Cr(VI) in COPR waste through wet detoxification, high temperature reduction, electro-kinetic remediation and solidification/stabilization (Asavapisit et al., 2005; Lehoux et al., 2017; Xu et al., 2011; Yoon

* Corresponding authors. State Key Laboratory for coal mine disaster dynamics and control, Chongqing University, Chongqing, 400044, PR China.

E-mail addresses: shawwong@126.com (X. Huang), j.binquan@cqu.edu.cn (B. Jiao), 158085585@qq.com (L. Yu), lironwei@cqu.edu.cn (D. Li).

et al., 2010). Among these technologies, solidification/stabilization is regarded as one of best available remediation technology that had been widely used for treatment of 57 types of hazardous wastes since 1970s (Batchelor, 2006).

Solidification/stabilization is the immobilization of heavy metals/hazardous wastes by physical and chemical ways in various cementing materials/binders (Qian et al., 2006; Shi and Fernández-Jiménez, 2006). The alkali activated cementitious materials/geopolymers are regarded as green cementing materials as compared to Ordinary Portland Cement (OPC) (Duxson et al., 2007). In addition, these 3rd generation of cementitious materials have high durability even in acidic environment and fire resistant surface than OPC (Muhammad et al., 2018). Based on these properties, alkali activated cementitious materials have also been used as alternatives of cement for construction purposes. While, low permeability and high mechanical strength are the main properties which allow these materials to be used for solidification of heavy metals/hazardous wastes (Huang et al., 2018; Meng et al., 2019).

The pozzolanic/cementitious behavior of inorganic materials having aluminosilicate composition are used for preparation of alkali activated cementitious materials such as coal gangue, blast furnace slag (BFS), clays, fly ash and calcined kaolin etc. These materials are activated by mixing with alkaline solutions (Xia et al., 2019). The alkaline solutions are prepared by dissolving NaOH, Na₂SiO₃, NaOH modified with Na₂SiO₃, KOH and K₂SiO₃ in water (Gao et al., 2017; Zhuang et al., 2016). As a result of activation, these aluminosilicate materials are dissolved into their reactive precursors i.e. Al³⁺ and Si⁴⁺. After dissolution, these ions are rearranged to give rise gelation, hardening and crystallization processes (Juenger et al., 2011). Regarding gelation, two kinds of gels i.e. N-A-S-H and C-(A)-S-H are formed depending upon nature of source material. The N-A-S-H is a sodium aluminosilicate gel resulted from alkaline activation of fly ash and metakaolin. In contrast, alkaline activation of BFS caused the dissolution of Ca and precipitation of Al to form C-(A)-S-H which is calcium aluminosilicate gel (Gao et al., 2015). Within one system, these two gels give rise formation of (N, C)-A-S-H gels by partially replacing Na with Ca. Consequently, these integrated gels can reduce and enhance the setting time and mechanical properties of these cementitious material, respectively (Gao et al., 2015). Therefore, these two source materials i.e. BFS and metakaolin are used for synthesis of geopolymer and solidification of COPR.

The number of authors have reported the solidification/stabilization of Cr(VI) either from chromium salt or from COPR wastes (Deja, 2002; Gao et al., 2017; Giergiczny and Król, 2008; Jagupilla et al., 2015; Nikolić et al., 2017; Zhang et al., 2008, 2017). Various kinds of binders including OPC and geopolymers are used for this purpose. The (Huang et al., 2017) had found that effect of geopolymers on Cr(VI) immobilization was better than OPC during stabilization of COPR. While (Zhang et al., 2008), had used fly ash based geopolymer to solidify Cr, Pb and Cd. Comparatively, the Cr(VI) immobilization was problematic. In another study (Palomo and Palacios, 2003), had examined that 2.6% addition of Cr(VI) resulted in complete failure of geopolymer setting. The (Muhammad et al., 2018) had also studied the effect of geopolymers on solidification of Cr(VI) by using three different concentrations (0.1%, 0.3% and 0.5%) on weight bases and found that just 0.1% of Cr(VI) could be successful stabilized without surpassing recommended concentrations. In addition, the solidification efficiency was more than 91% at all Cr(VI) levels but had surpassed the critical limits. These all studies showed that geopolymer can stabilize the Cr(VI) up to some extent but still its solidification is problematic. Therefore, it is considered that effective stabilization of Cr(VI) could be achieved after its conversion/reduction to Cr(III). Several kinds of organic and inorganic (iron and sulfur) based reducing agents had

been used for this purpose (Su and Ludwig, 2005).

Recently, the iron based reducing agents especially zerovalent (Huang et al., 2018; Li et al., 2015) and nano zerovalent iron (NZVI) (Du et al., 2012) had been widely used due to its economic value and abundant in nature. The NZVI particles are synthesized by biological, physical and chemical ways (Shahwan et al., 2011). Among them, physical and chemical techniques are efficiently used to produce nanoparticles but have several limitations such as toxic and flammable in nature, large cost due to high amount of energy (Kumar et al., 2015). Thus, green or eco-friendly technologies are required to overcome these problems. The several scientists have synthesized NZVI particles with plant materials/extracts and used it for remediation of industrial or waste water contaminated with various heavy metals including chromium (Fazlzadeh et al., 2017; Kumar et al., 2015; Mystrioti et al., 2014). Although (Du et al., 2012), had used commercially or traditionally synthesized nano zerovalent iron for reduction of chromium to stabilize it into geopolymer matrices and achieved satisfactory results. To best of authors knowledge, there is no work recently carried out to solidify the pretreated Cr(VI) with plant synthesized NZVI in alkali activated cementitious materials.

The Cr(VI) in COPR was pretreated with green tea mediated NZVI and its solidification in composite based alkali activated cementitious material was carried out in this experiment. The key objectives of this study were; (1) synthesis of NZVI particles with green tea (GT-NZVI) and its characterization, (2) effect of GT-NZVI particles, acid dosage and time duration on reduction of Cr(VI) existed in COPR, (3) the Cr immobilization present in COPR slurry treated with GT-NZVI and untreated COPR slurry through composite based geopolymer (BFS and MK) and (4) the characterization and solidification/stabilization mechanism analysis of solidified bodies i.e. GCM-(GT-NZVI) and GCM.

2. Materials and methods

2.1. Source materials and chemicals

The origin source of Chromite ore processing residue (COPR) was chemical factory (Chongqing province, China). The BFS from steel plant utilized in this experiment was also collected from Chongqing province, China. The kaolin powder bought from Sinopharm Chemical Reagent Co., Ltd, (Shanghai province, China) was subjected to calcination temperature (750 °C) for 3 h to produce MK. While, oolong green tea was purchased from Anxi, Fujian province, China. The liquid water glass (silicate modulus 3) and sodium hydroxide were technical and analytical grades respectively.

2.2. Methodology

2.2.1. Synthesize of green tea nano zerovalent iron particles (GT-NZVI)

The GT-NZVI particles were previously synthesized by (Huang et al., 2014). The small pieces of green tea were washed with tap water to remove the dust and dried at 60 °C in oven for 2 h. The green tea extract was vacuum filtered after boiling 60 g/l leaves of green tea at 80 °C for 1 h. Afterwards, the 0.1 M FeSO₄·7H₂O solution was added into 60 g/l tea leaves extract in ratio of 2:3. The pH value was adjusted to 6 by adding 1 M NaOH. Consequently, black colored precipitates were appeared which confirmed the formation of GT-NZVI particles. The formed nanoparticles were separated by evaporation on a hot plate surface. The separated GT-NZVI particles were washed three times with 1 M ethanol solution through centrifugation at 6000 rpm. The washed GT-NZVI particles were dried in oven at 60 °C overnight and placed in airtight bags to avoid oxidation.

2.2.2. Prereduction experiment

The Cr(VI) was extracted from COPR. For this purpose, 10 g of COPR in certain volume of water was stirred mixture for 25 min. The stirred mixture was kept for 10 min to be settled. Afterwards, the suspension was filtered and initial Cr(VI) contents were determined. The separated COPR slurry was saved. In filtrate, certain amount of GT-NZVI and volume of 0.1 M H₂SO₄ were added. This mixture was kept for certain period of time to carry out the reaction. The saved COPR slurry was again mixed with filtrate and kept for certain period of time so that remaining Cr(VI) in slurry could also react with GT-NZVI. The Cr(VI) was determined after filtration of mixture having reacted filtrate and saved slurry.

2.2.3. Solidification/stabilization of COPR in geopolymer matrix

The BFS was sieved through 200 mesh and mixed with meta-kaolin for 4 min to obtain homogeneous mixture. The mass ratio of BFS and MK was 9:1. This composite material was mixed with alkali activator solution until dense paste is achieved. The activator solution was synthesized by mixing NaOH and water glass by maintaining the ratio of 3:7 (on basis of solid constituents) in deionized water. The alkali activator to composite material ratio was 1:9. While, liquid to solid ratio was 0.25. The dense paste achieved after mixing composite material with alkaline activator solution that was added into the cubic moulds (dimension of 20 mm × 20 mm × 20 mm) and kept on vibrator to remove air bubbles. The samples were de-moulded after curing at 35 °C for 24 h. Later, samples were kept under constant temperature of 26 °C in oven. The samples were watered after regular interval of 5–7 days to keep the surface moist for 28 days. Regarding COPR solidification, various contents of GT-NZVI treated (according to section 2.2.1) and untreated COPR were introduced into colloids during their synthesis.

2.3. Leaching experiment

Two different Chinese leaching extractant protocols i.e. HJ/T 300–2007 and HJ/T 557–2010 were utilized to evaluate leaching behavior as carried out by (Muhammad et al., 2018). The solidified products with COPR were crushed and granular materials having size <9.5 mm were used for leaching analysis in both methods. The acetic acid solution having pH 2.88 ± 0.05 was prepared in HJ/T 300–2007 standard. In this method, the granular materials were stirred for 16 h by keeping the liquid to solid ratio of 20. While, granular materials were stirred for 8 h in deionized water by maintaining the liquid to solid ratio of 10 in HJ/T 557–2010 method. After stirring, solution was kept for 16 h and then Cr was determined.

2.4. Characterization analysis

The GT-NZVI particles were analyzed under Transmission electron microscope equipped with EDS and Scanning Electron Microscope (SEM, TESCAN, Czech). The mineral phase and functional group were analyzed through X-ray diffraction (XRD, Shimadzu, Japan) and Fourier-Transform Infrared Spectroscopy (FTIR, Thermo Nicolet Corp, USA), respectively.

The solidified products (three replicates of each sample) were subjected for compressive strength analysis which was determined through universal testing machine (AGN-250, Shimadzu, Japan). The total Cr was determined in accordance with Chinese Standard HJ 749–2015 by flame atomic absorption spectrophotometer (Huang et al., 2018). While, Cr(VI) was determined by 1,5-diphenylcarbohydrazide spectrophotometric method (Chinese Standard GB/T 15555.4–1995) (Huang et al., 2018). The COPR samples were tested for X-ray fluorescence (XRF, Shimadzu, Japan). The

microscopic alterations, crystallinity and molecular composition was analyzed by SEM-EDS (Carl Zeiss AG, Germany), XRD and FTIR respectively. The chemical composition of raw materials used in preparation of composite based geopolymer and solid waste i.e. COPR are presented in Table 1.

3. Results and discussion

3.1. Characterization analysis of GT-NZVI

The morphology and physical appearance of GT-NZVI particles was examined through SEM. The successful synthesis of NZVI particles could be seen in SEM images (Fig. 1), having irregular shapes and varying sizes. These varying sizes were inherited from various natural compounds in green tea which have different reducing properties (Wang et al., 2014a).

The further confirmation and composition of green tea synthesized NZVI were subjected to TEM analysis equipped with EDS. The TEM images are shown in Fig. 2. The well dispersion among particles could be seen in Fig. 2 (a) and (b). The dispersion among particles was attributed to presence of polyphenols in green tea extracts which served as capping agent. The EDS spectrum (Fig. 2 (c)) analysis showed the peaks of Fe, C, O, K, S and Na. This elemental analysis had confirmed the presence of Fe. The existence of C and O were ascribed to polyphenolic groups and other aromatic groups in green tea or plant leaves extracts (could be seen in FTIR analysis) (Kuang et al., 2013; Santos et al., 2012). The K and S might be originated from oolong tea extracts which were also observed by (Huang et al., 2014) when they were synthesizing the NZVI particles from oolong tea extract. While Na must be arisen from NaOH which was utilized during the synthesise of NZVI in maintaining the pH.

The XRD peaks of GT-NZVI particles are shown in Fig. 3. The GT-NZVI particles were amorphous in nature which were also observed by (Hoag et al., 2009; Shahwan et al., 2011) during synthesis of NZVI by plant extracts. In addition, some peaks correspondent to iron oxide (PDF# 76–1470) and magnetite (PDF # 74–1910) were analyzed at 15°, 22° and 30°, 47° of 2θ, respectively. The iron oxides were also noted by (Huang et al., 2014) during synthesis of GT-NZVI.

The probable biomolecules responsible for synthesise of GT-NZVI particles were identified through FTIR analysis (Fig. 4). The wavenumber of 3250 cm⁻¹ was correspondent to phenolic groups or O–H stretching vibrations which were also reported in literature roundabout at wave numbers of 3200–3500 cm⁻¹ (Devatha et al., 2016; Fazlzadeh et al., 2017; Wang et al., 2014b). It is stated by (Madhavi et al., 2013) that these polyphenols are responsible for

Table 1

The chemical composition of BFS, Mk and COPR (mass, %).

Elements	BFS	MK	COPR
SiO ₂	35.62	55.12	2.60
Al ₂ O ₃	14.93	41.78	26.10
Fe ₂ O ₃	0.67	0.43	41.91
CaO	36.31	0.17	0.23
TiO ₂	1.28	0.17	1.31
Na ₂ O	0.22	0.35	3.39
SO ₃	2.29	–	0.14
K ₂ O	0.39	0.17	–
MgO	7.50	0.09	10.16
MnO	0.69	–	–
P ₂ O ₅	–	0.43	–
Cr ₂ O ₃	–	–	13.35
V ₂ O ₅	–	–	0.34
NiO	–	–	0.17
ZnO	–	–	0.14

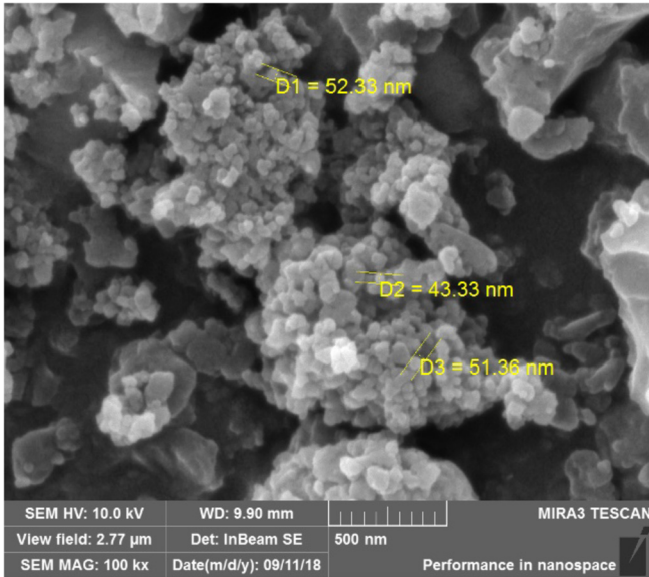


Fig. 1. SEM image of GT-NZVI.

reduction of Fe(II) to Fe(0). The C–N stretching (aromatic amines) vibrations were analyzed at wave number of 362 cm^{-1} (Wang et al., 2014a). The FTIR stretching vibrations at 1622 cm^{-1} and 1074 cm^{-1} were parallel to absorption peaks of C=C and C–O–C (Wang et al., 2014b). While, absorption bands of 816 cm^{-1} and 600 cm^{-1} were C–H bending of aromatic and alkanes (acetylene) compounds, respectively (Fazlzadeh et al., 2017). The above mentioned amino or carboxylic groups are responsible for stabilization of GT-NZVI particles (Das et al., 2010; Mohan Kumar et al., 2013). The presence of 420 cm^{-1} vibration considered as Fe–O stretches of Fe_2O_3 which was resulted from oxidation of Fe nanoparticles upon being exposed to air or water (Wang et al., 2014b), and it was consistent with XRD results.

3.2. Prereduction experiment

In this section, three factors i.e. reaction time, GT-NZVI and acid dosage were used to treat the 10 g of COPR so that best ratio of each factor could be achieved and used in solidification experiment.

3.2.1. Effect of reaction time

The Cr(VI) containing COPR was treated for six different time intervals. While, the dosage of NZVI (0.7%) and acid ($0.8\text{ mol H}^+/\text{Kg}$

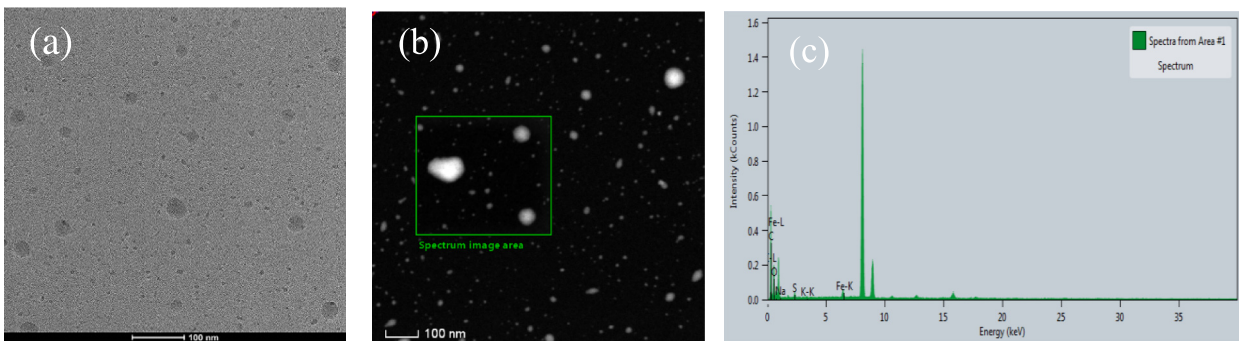


Fig. 2. TEM of GT-NZVI

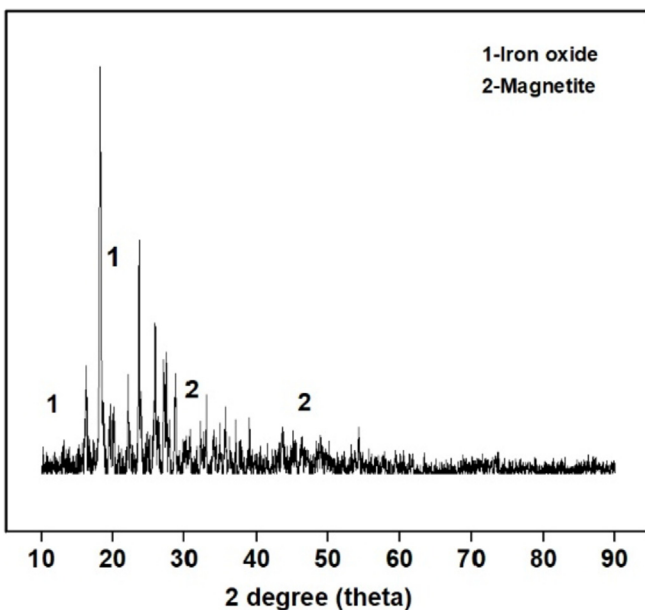


Fig. 3. XRD pattern of GT-NZVI.

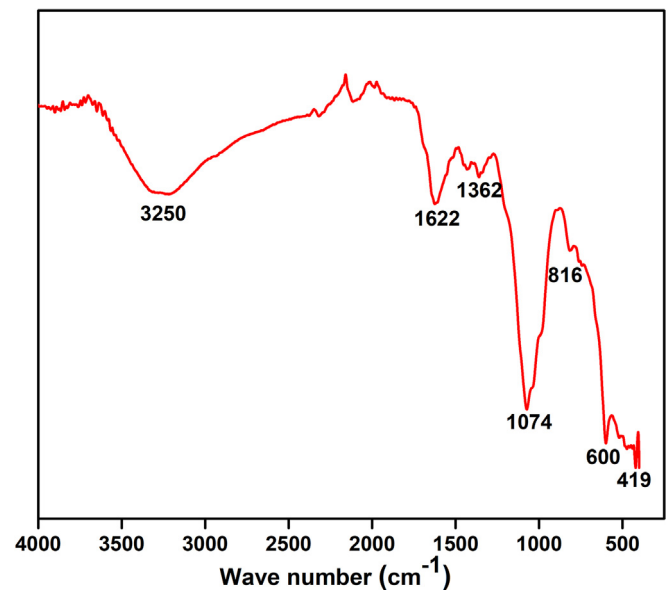


Fig. 4. FTIR peaks of GT-NZVI.

COPR) were constant (Fig. 5 (a)). Each time interval is divided into two equal halves. In first half interval, the reduction reaction was carried out in filtrate. While, slurry was added in second half interval so that time could be effectively used. For example, the reaction was carried out for 36 min; in which first 18 min the filtrate was treated and next 18 min the slurry was added in to the filtrate to carry out the reduction process. The Cr(VI) concentration decreased with passage of time and no Cr(VI) was detected after being treated for 18 min. This indicate that enough time is required by GT-NZVI which could effectively reduce the Cr(VI). Similar findings were observed by (Fazlzadeh et al., 2017) when they were utilizing the plant synthesized NZVI for treatment of Cr(VI).

3.2.2. Effect of acid dosage

Basically, COPR is a high pH waste which lowers the reduction capability of ZVI (Huang et al., 2018). Therefore, COPR was treated with different acid dosages for 18 min while keeping the constant dosage of GT-NZVI (0.7%) which could be seen in Fig. 5(b). The Cr(VI) concentration was decreased from 98.56 to 37.93 mg/L with addition of 0.2–0.4 mol H⁺/Kg COPR dosage of acid. While, no Cr(VI) was detected when the acid dosage was 0.6–1.2 mol H⁺/Kg COPR. These results indicated that minimum dosage of 0.6 mol H⁺/Kg COPR is enough for complete reduction of Cr(VI) in slurry. The (Huang et al., 2018; Li et al., 2015) had also analyzed that Cr(VI) reduction in slurry increased with increasing the acid dosage. It was because of existence of high soluble Cr(VI) species e.g. HCrO₄⁻, Cr₂O₇²⁻, Cr₃O₁₀²⁻, Cr₄O₁₃²⁻ and CrO₄²⁻ at low pH which can easily adsorb and react with NZVI (Fazlzadeh et al., 2017; Levankumar et al., 2009; Yuan et al., 2009).

3.2.3. Effect of GT-NZVI dosage

Effect of different NZVI contents/dosages (0.1–1.1% of COPR mass (10 g)) on Cr(VI) are presented in Fig. 5(c). While, the reaction time of 18 min and acid dosage of 0.8 mol H⁺/Kg COPR were constant. Similar to other two factors (time and acid dosage), the Cr(VI) concentration decreased with increase of GT-NZVI content. Small decrease (289–265.7 mg/L) in Cr(VI) concentration was observed with 0.1% addition of GT-NZVI. In addition, the sudden decrease of 76.6 to 4.9 mg/L in Cr(VI) concentration was observed with addition of 0.3–0.5% of GT-NZVI. While, the Cr(VI) was completely vanished upon addition of 0.7% or higher dosage of GT-NZVI. It was due to the fact that higher the GT-NZVI dosage, higher the available reactive surface which lead to higher reduction of Cr(VI). Similar reason was explained by (Wang et al., 2013) when they were using bentonite supported bimetallic (Fe/Pb) nanoparticles for treatment of methyl orange contaminated water. Regarding NZVI dosage, the (Du et al., 2012) had used 6% of NZVI particles for reduction of Cr(VI) (92.1 mg/L) and (Huang et al., 2018) had used 1.2% of ZVI particles for reduction of 59 mg/L of extracted Cr(VI) in COPR. However, the 0.7% of GT-NZVI were enough for complete reduction of Cr(VI) (289 mg/L) present in COPR in current study.

The possible Cr(VI) reduction mechanism could be explained as; (a) Cr(VI) adsorption on surface of GT-NZVI, (b) oxidation of Fe⁰ to Fe²⁺ which react with Cr(VI) and reduce it into Cr(III). Consequently, continuous reduction of Cr(VI) leads to precipitation of Fe²⁺ and Fe²⁺ oxidized into Fe³⁺. Resultant Fe³⁺ and Cr(III) are precipitated in alkaline environment (after mixing the extraction solution with COPR slurry which had high pH buffering capacity).

3.3. Solidification/stabilization experiment

3.3.1. Compressive strength

The compressive strength is a vital parameter, usually used to evaluate the suitability of cementitious binders/solidified bodies for construction purposes and also used for effectiveness of

solidification technology. Hence, the compressive strength of alkali activated cementitious bodies/geopolymer containing COPR was determined. Generally, the similar trend in compressive strength was observed while stabilization of treated (GT-NZVI) and untreated COPR samples (Fig. 6). The compressive strength of solidified bodies (GCM-(GT-NZVI) and GCM increased up to certain addition of COPR then decreased with further increase of COPR content. The increase in strength as compared to control samples might be due to varying size of particles (BFS, MK and COPR) which acted as filler (Jaturapitakkul et al., 2011). Another reason might be physical encapsulation of Cr(VI) in COPR waste because the physical encapsulation have better mechanical strength as compared to chemical interactions (Guo et al., 2017). In addition to physical encapsulation, decrease in strength at higher addition of COPR attributed towards chemical interaction of Cr(VI) with gel phases. Comparatively, the compressive strength of GCM-(GT-NZVI) solidified bodies was lower as compared to GCM. In contrast (Huang et al., 2018), work indicated that compressive strength of solidified samples having ZVI treated COPR was higher as compared to untreated samples. In present study, the lower strength of GT-NZVI treated samples was might be due to plant synthesized NZVI particles which were bounded by organic material especially organic acid released from plant extract (Fazlzadeh et al., 2017). The (Tastan Erdem et al., 2011) had cited that calcium ions in binder were consumed by organic acids until acid neutralization and then remaining calcium ions take parts in gel phase genesis and strength development. Up to 50% addition of COPR, the compressive strength of GCM-(GT-NZVI) and GCM solidified bodies was greater than 33 and 47 MPa respectively. These results indicated that GCM-(GT-NZVI) and GCM solidified bodies could be potentially used for construction and landfill purposes because their required strength is > 10 MPa (Huang et al., 2018) and 0.35 MPa (Malaviya and Singh, 2011; Malviya and Chaudhary, 2006) respectively.

3.3.2. Leaching experiment

Similar to compressive strength, leaching behavior is another important parameter to examine the suitability of solidification/stabilization technology. Generally, total Cr and Cr(VI) in both methods (HJ/T 300–2007 and HJ/T 557–2010) were lower in GCM-(GT-NZVI) samples as compared to GCM samples (Fig. 7). According to GB 5085.3–2007 standards, GCM-(GT-NZVI) and GCM were not identified as hazardous materials because total Cr and Cr(VI) had not exceeded the safe limits (Table 2). In GCM-(GT-NZVI) samples, total Cr and Cr(VI) were in range of 0.23–1.2 mg/L and 0.030–0.18 mg/L respectively in HJ/T 300–2007 method. While, this range was 0.2–0.9 mg/L (total Cr) and 0.029–0.21 mg/L in HJ/T 557–2010 method. According to standards defined in Table 2, GCM-(GT-NZVI) samples up to 30% addition of COPR could be utilized for building blocks and bricks. In addition, it could be utilized as source materials for roadbed and concrete aggregate up to 40% addition of COPR. Additionally, all samples could be subjected for different kinds of landfills (Table 2).

Regarding untreated GCM samples, total Cr was in range of 0–1.8 mg/L and Cr(VI) was in range of 0.44 mg/L respectively in HJ/T 300–2007 method. In HJ/T 557–2010 method, total Cr and Cr(VI) were in range of 0.4–2 and 0.03–0.3 mg/L. In GCM samples, all samples could be utilized for landfill purposes (Table 2) and samples only having 10% COPR could also be utilized for building blocks and bricks. These samples up to 20% addition of COPR could also be subjected for preparation of roadbed and concrete aggregates. In addition, the leaching concentration increased with addition of higher amount of COPR in both GCM-(GT-NZVI) and GCM samples due to lower compressive strength. As explained by (Muhammad et al., 2018), lower the strength higher will be leaching.

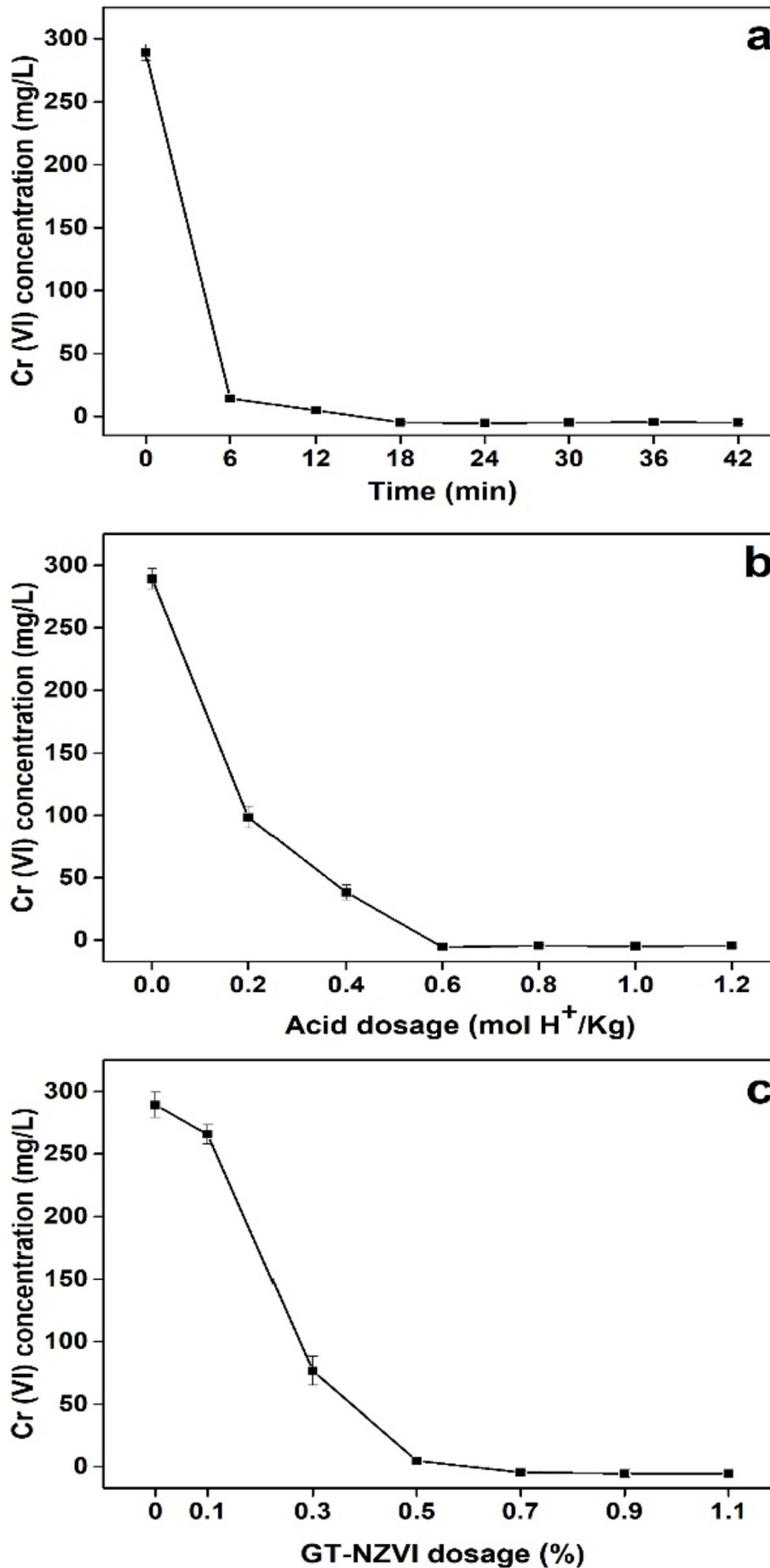


Fig. 5. Effect of various factors on Cr(VI) reduction.

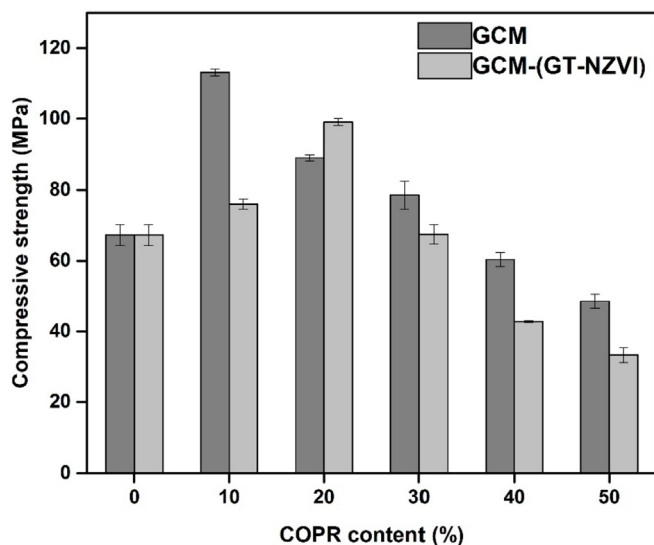


Fig. 6. The compressive strength of GCM and GCM-(GT-NZVI).

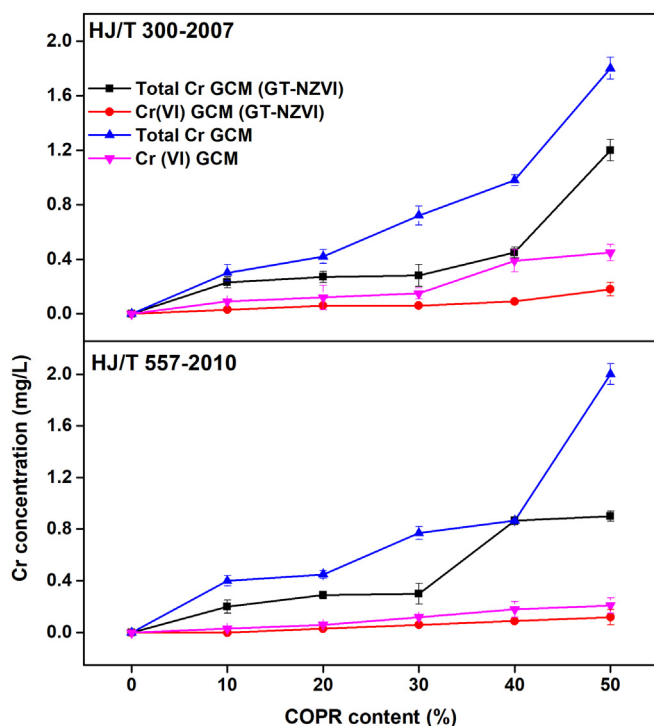


Fig. 7. The HJ/T 300–2007 and HJ/T 557–2010 leaching tests of GCM and GCM (GT-NZVI).

Table 2
The safe limits of total Cr and Cr(VI) (mg/L)(Huang et al., 2018).

Standard protocols	Applications	Total Cr	Cr(VI)
GB 5085.3–2007	Hazardous wastes identification	15.0	5.0
HJ/T 301-2007	Manufacturing of building blocks and bricks.	0.3	0.1
	Utilized as source materials for roadbed and concrete aggregate.	1.5	0.5
	Disposal in municipal solid waste landfill	4.5	1.4
	Disposal in general industrial solid waste landfill	9.0	3.0
TCLP	Sanitary landfill disposal		5.0

3.3.3. Characterization analysis of solidified bodies

3.3.3.1. X-ray diffraction analysis. The mineral phase analysis of raw source materials i.e. BFS, K and MK utilized for preparation of geopolymer and COPR waste are presented in Fig. 8. In BFS, no distinct phases were observed but weak and broad peaks around 25°-35° 2θ were found which indicated that it was an amorphous material. While, the COPR was dominated with magnesium chromium oxide (PDF# 20–0673). The kaolin had poor crystals of kaolinite (PDF# 20–1488) and very few mullite phases. While, the number of weak mullite phases (PDF# 74–1784) increased in MK after calcination temperature.

After alkaline activation, the notable changes were observed in XRD pattern of solidified samples without COPR waste (GCM) as compared to raw materials (Fig. 9). The shifting of BFS amorphous hump at higher angle in GCM samples indicated that new amorphous phases were formed. In addition, the gehlenite (PDF# 74–1607) and N-A-S-H based albite phases (PDF# 09–0456) (Ranjbar et al., 2014) were also observed in GCM samples. The albite phases might be formed due to alkaline activation of two different sources of materials i.e. BFS and MK which have different gel phases. These peaks were disappeared in solidified samples having untreated (GCM-50) and zerovalent treated (GCM-50(GT-NZVI)) COPR. In GCM-50 samples, the sharp peaks were reflections of magnesium aluminium iron oxide (PDF# 11–009), which were formed due to COPR interaction with geopolymer. The (Huang et al., 2017) had also observed the similar findings during stabilization of COPR. While, the magnetite (PDF# 75–0449) remained unreacted in GCM-50 (GT-NZVI) samples which was also observed in XRD pattern of GT-NZVI (Fig. 3). It might be because of plant material which were bounded on NZVI. This was the main reason of lower strength of GT-NZVI samples as compared to GCM samples because the organic acids on GT-NZVI had neutralizing effect on calcium ions. In both GCM-50 and GCM-50 (GT-NZVI) samples, the absence of Cr containing phases indicated that Cr was bounded in amorphous phases of aluminosilicate (Huang et al., 2018).

3.3.3.2. FTIR analysis. The FTIR bands and corresponding species of GCM, GCM-50 and GCM-50 (GT-NZVI) samples are show in Fig. 10 and Table 3. The FTIR bands of 3314 and 1646 cm⁻¹ were correspondent to H–O–H bonds which indicated the existence of water (H₂O) in samples (Muhammad et al., 2018). Moreover, the asymmetric stretching vibrations of Si–O–Al (Si) were observed in range of 946–952 cm⁻¹ (Wang et al., 2018). This showed that geopolymerization resulted in formation of Al–O and Si–O bonds. The stretching band (946 cm⁻¹) in GCM sample (without COPR waste) was influenced by addition of COPR waste. This band was shifted from 946 cm⁻¹ to 950 cm⁻¹ and 952 cm⁻¹ with addition of 50% of treated and untreated COPR waste. This shifting of bands to higher wavenumber had evidenced that Si–O–Al(Si) system was influenced by Cr interaction present in COPR waste. In addition, the geopolymer had amorphous crystals (discussed in XRD section) which constituent Al and Si tetrahedral units, each surrounded by four O₂ atoms. Consequently, the net -VE charge developed in geopolymer structure because Al³⁺ is surrounded by four

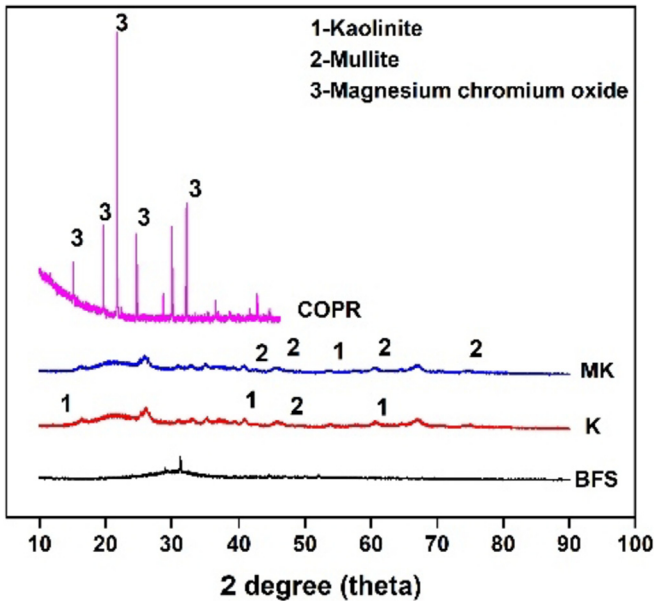


Fig. 8. The XRD pattern of raw materials.

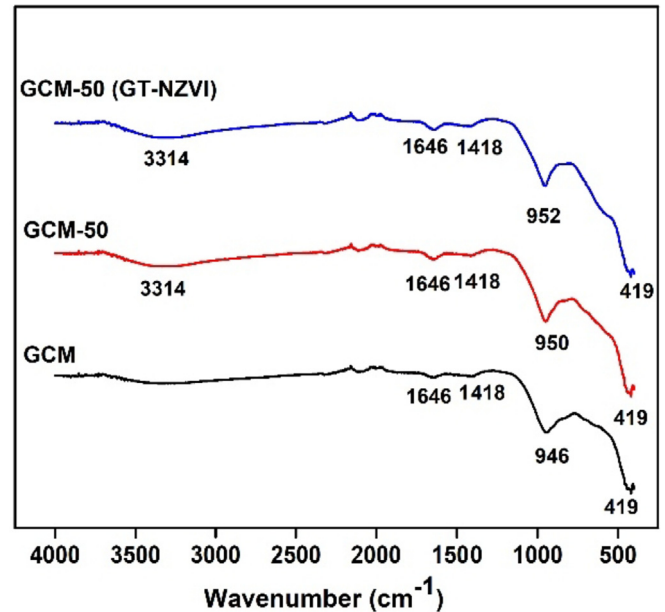


Fig. 10. The FTIR peaks of solidified products.

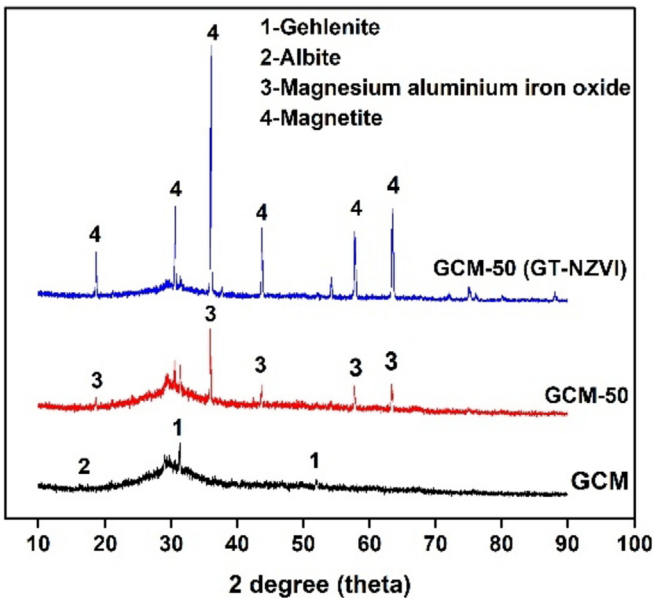


Fig. 9. The XRD pattern of solidified products.

negatively charged oxygen atoms. In this situation, Na^+ and Ca^{2+} ions which had already satisfied the charge get replaced with Cr situated in COPR waste. In this way, the Cr was stabilized in geopolymer system. Regarding GCM-50(GT-NZVI) samples, the GT-NZVI nanoparticles were bounded by polyphenols or other organic aromatic compounds which had hindered the geopolymerization reaction because these remain unreacted also verified by XRD pattern. Therefore, higher shift in stretching band of 946 cm^{-1} was observed in GCM-50(GT-NZVI) samples as compared to GCM-50. In addition, the shift of stretching band of 946 cm^{-1} had confirmed that geopolymer structure was disturbed and resulting in decrease of compressive strength and increase of leaching content.

Table 3

FTIR bands and corresponding species of composite based geopolymer.

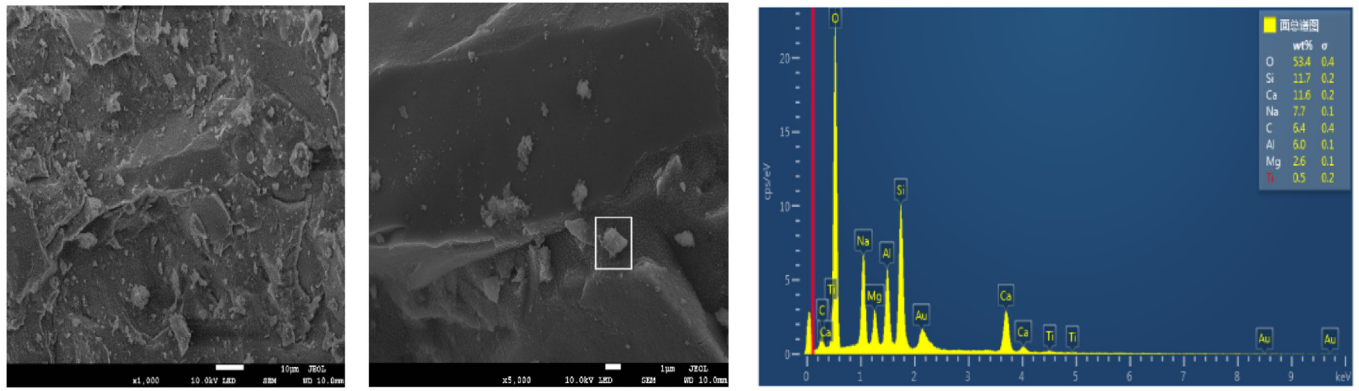
Types of species	FTIR bands (cm^{-1})
H–O–H bending	1600–1700, 3000–4000
Asymmetric stretching of Si–O–Al (Si)	900–1000
Stretching vibration of O–C–O	1418
Bending vibration of Si–O–Si and O–Si–O	400

3.3.3.3. SEM/EDS analysis. The SEM micrographs along with elemental map are presented in Fig. 11. It could be seen that control samples (GCM) had more compacted and dense structures (Fig. 11 (a)) as compared to GCM-50 (Fig. 11(b)) and GCM-50 (GT-NZVI) (Fig. 11(c)). The more compacted structure might be due to formation of high number of gels. According to spot elemental map analysis, the presence of Na, Al, Ca and Si had confirmed the formation of (N, C)-A-S-H gels which were previously reported by (Huang et al., 2018) and also observed in XRD analysis. The GCM-50 (GT-NZVI) have more abrasions as compared to GCM-50 samples. It might be due to presence of organic compounds on NZVI particles which were released from tea extract and its also could be seen from elemental map of spot analysis of GCM-50 (GT-NZVI) sample which had higher concentration of carbon. In addition, the presence of lower content of calcium element in GCM-50 (GT-NZVI) as compared to GCM-50 samples had also indicated that calcium was consumed by organic acid present on GT-NZVI and consequently the lower strength was observed in GCM-50 (GT-NZVI).

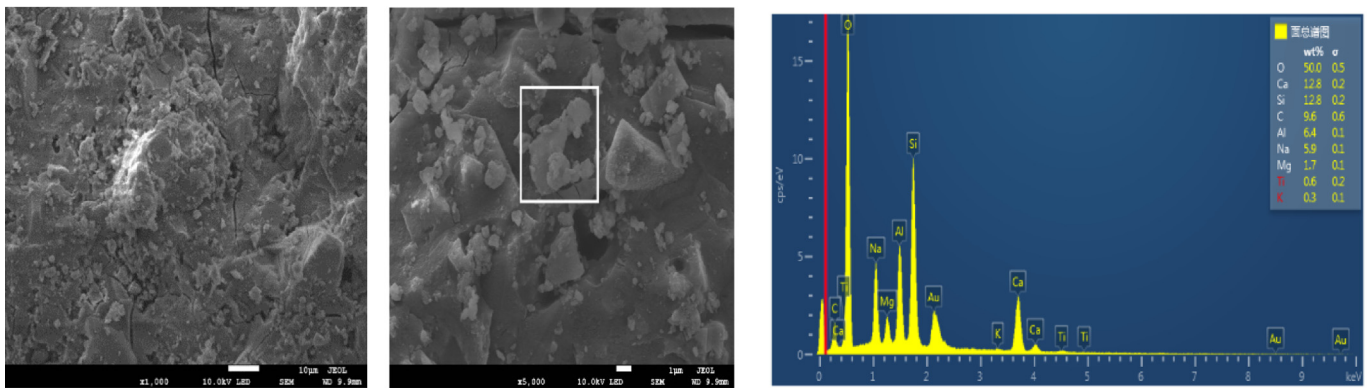
3.4. Mechanism analysis

3.4.1. Geopolymerization

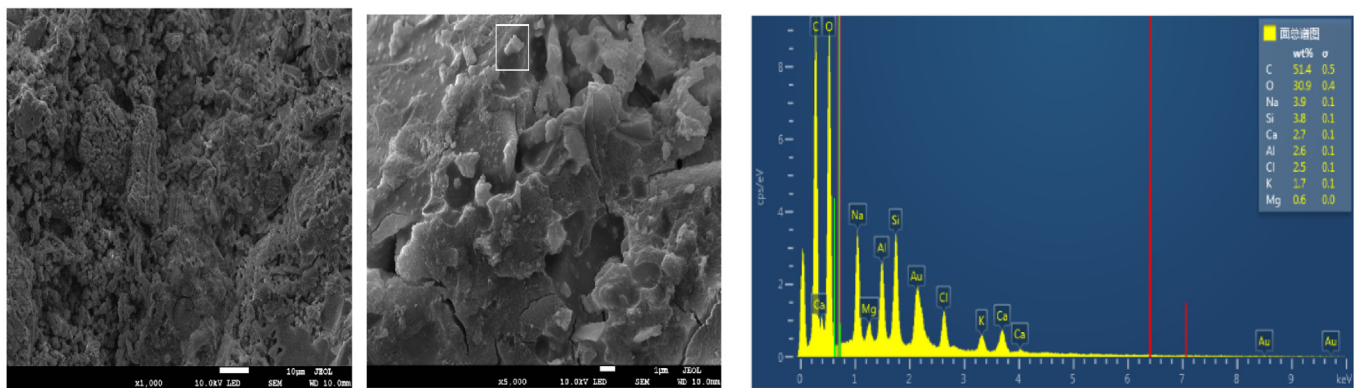
The raw BFS and MK were used as source material for solidification/stabilization of Cr(VI) in COPR waste. According to XRD analysis, both materials were amorphous in nature with low crystallinity. The dissolution of BFS and MK into their precursors i.e. Ca^{2+} , $[\text{SiO}_4]^{4-}$ and $[\text{AlO}_4]^{5-}$ after addition of alkaline activator leads to rearrangement of these ionic species. The rearrangement and interaction among Ca^{2+} , $[\text{SiO}_4]^{4-}$ and $[\text{AlO}_4]^{5-}$ leads to formation of C-(A)-S-H gel (Huang et al., 2018; Muhammad et al., 2018). While,



(a)



(b)



(c)

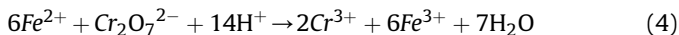
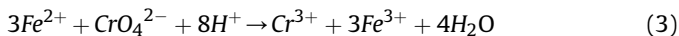
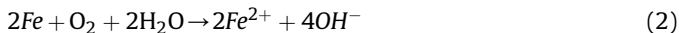
Fig. 11. SEM and EDS images of (a) control samples (b) GCM-50 (c) GCM-50 (GT-NZVI).

amorphous aluminosilicate structures were formed as result of further polymerization between Al and Si units. The hardened and compacted structures as result of geopolymerization could also be analyzed in SEM images. Moreover, formation of albite phase was also detected which had sodium (Na^+) ion in its structure and lead to formation of N-(A)-S-H gel. The FTIR analysis had also showed that geopolymer was composed of Si–O–Al (Si) system.

3.4.2. Reduction

Regarding reduction mechanism, it was reported in several studies that smaller quantities of S^{2-} ions also existed in BFS which could reduce the little amount of Cr(VI). Therefore, the addition of reducing agents are required to achieve the better results. Basically, the H^+ ions react with Fe^0 and get oxidized into Fe^{2+} in presence of dissolved oxygen which could be seen in Eq. (1) and Eq (2). The is Fe^{2+} further oxidized in to Fe^{3+} by reducing Cr^{3+} in accordance

with Eq. (3) and Eq. (4).



3.4.3. Immobilization

Immobilization is possibly carried out through physical encapsulation and chemical bonding. The increase in strength up to certain addition of COPR in both GCM and GCM (GT-NZVI) samples as compared to control might be due to physical encapsulation. Another, physical mechanism is possible through charge balancing; the net negative charge on geopolymer is balanced by Cr^{3+} and Fe^{3+} after replacing already balancing ions i.e. Ca^{2+} and Na^+ (Muhammad et al., 2018; Shi and Fernández-Jiménez, 2006). Furthermore, the chemical interaction was also verified through disturbance in wavenumber of 946 cm^{-1} which was correspondent to Si–O–Al (Si) bonds (Muhammad et al., 2018). The chemical immobilization could also be analyzed through Cr(VI) leaching in aggressive environment (Zhang et al., 2008) i.e. HJ/T 300–2007 method which had acetic acid. According to above discussion the Cr(VI) had not exceeded the safe limits in aggressive environment.

4. Conclusions

Since last few decades, the solidification/stabilization technique through industrial byproducts has gained popularity in term of its economic cost and environmental impact. In this study, the COPR was pretreated with green tea synthesized nano zerovalent iron(GT-NZVI) particles for effective immobilization of Cr(VI) in composite based geopolymer. Following conclusions were drawn:

1. The reduction of Cr(VI) in COPR was examined under different dosages of GT-NZVI particles, acid dosages and time intervals. The effective reduction of Cr(VI) could be achieved by treating the COPR for 18 min with 0.7% of GT-NZVI and acid dosage of $0.6\text{ mol H}^+/\text{Kg}$.
2. Compressive strength of GT-NZVI solidified bodies were lower as compared to untreated COPR because of capping of GT-NZVI particles with organic compounds especially organic acids which consume the calcium ions until acid neutralization. This was role of GT-NZVI particles on mechanical properties of solidified bodies.
3. Although the Cr(VI) did not exceed toxicity limits in both treated and untreated COPR samples but GT-NZVI treated could be utilized in several applications such as in preparation of building blocks and bricks (up to 30% addition of COPR). In addition, solidified samples having treated COPR (up to 40% addition) could be utilized for roadbed and concrete aggregates. While, solidified samples having untreated COPR could be used for building blocks and bricks up to 10% addition of COPR, and up to 20% addition could be used for preparation of roadbed and concrete aggregates.

Conflicts of interest

There are no conflicts of interest to declare.

Acknowledgement

This research did not receive any specific grant from funding agencies in the public, commercial, or not-for-profit sectors.

References

- Asavapisit, S., Naksrichum, S., Harnwajanawong, N., 2005. Strength, leachability and microstructure characteristics of cement-based solidified plating sludge. *Cement Concr. Res.* 35 (6), 1042–1049.
- Batchelor, B., 2006. Overview of waste stabilization with cement. *Waste Manag.* 26 (7), 689–698.
- Das, R.K., Borthakur, B.B., Bora, U., 2010. Green synthesis of gold nanoparticles using ethanolic leaf extract of *Centella asiatica*. *Mater. Lett.* 64 (13), 1445–1447.
- Deja, J., 2002. Immobilization of Cr^{6+} , Cd^{2+} , Zn^{2+} and Pb^{2+} in alkali-activated slag binders. *Cement Concr. Res.* 32 (12), 1971–1979.
- Dermatas, D., Chrysochoou, M., Moon, D.H., Grubb, D.G., Wazne, M., Christodoulatos, C., 2006. Ettringite-induced heave in chromite ore processing residue (COPR) upon ferrous sulfate treatment. *Environ. Sci. Technol.* 40 (18), 5786–5792.
- Devatha, C.P., Thalla, A.K., Katte, S.Y., 2016. Green synthesis of iron nanoparticles using different leaf extracts for treatment of domestic waste water. *J. Clean. Prod.* 139, 1425–1435.
- Du, J., Lu, J., Wu, Q., Jing, C., 2012. Reduction and immobilization of chromate in chromite ore processing residue with nanoscale zero-valent iron. *J. Hazard Mater.* 215–216, 152–158.
- Duxson, P., Fernández-Jiménez, A., Provis, J.L., Lukey, G.C., Palomo, A., van Deventer, J.S.J., 2007. Geopolymer technology: the current state of the art. *J. Mater. Sci.* 42 (9), 2917–2933.
- Fazlzadeh, M., Rahmani, K., Zarei, A., Abdoallahzadeh, H., Nasiri, F., Khosravi, R., 2017. A novel green synthesis of zero valent iron nanoparticles (NZVI) using three plant extracts and their efficient application for removal of Cr(VI) from aqueous solutions. *Adv. Powder Technol.* 28 (1), 122–130.
- Gao, X., Yu, Q.L., Brouwers, H.J.H., 2015. Reaction kinetics, gel character and strength of ambient temperature cured alkali activated slag–fly ash blends. *Constr. Build. Mater.* 80, 105–115.
- Gao, X., Yuan, B., Yu, Q.L., Brouwers, H.J.H., 2017. Characterization and application of municipal solid waste incineration (MSWI) bottom ash and waste granite powder in alkali activated slag. *J. Clean. Prod.* 164, 410–419.
- Giergiczny, Z., Król, A., 2008. Immobilization of heavy metals (Pb, Cu, Cr, Zn, Cd, Mn) in the mineral additions containing concrete composites. *J. Hazard Mater.* 160 (2), 247–255.
- Guo, X., Zhang, L., Huang, J., Shi, H., 2017. Detoxification and solidification of heavy metal of chromium using fly ash-based geopolymer with chemical agents. *Constr. Build. Mater.* 151, 394–404.
- Hoag, G.E., Collins, J.B., Holcomb, J.L., Hoag, J.R., Nadagouda, M.N., Varma, R.S., 2009. Degradation of bromothymol blue by 'greener' nano-scale zero-valent iron synthesized using tea polyphenols. *J. Mater. Chem.* 19 (45), 8671–8677.
- Huang, L., Weng, X., Chen, Z., Megharaj, M., Naidu, R., 2014. Synthesis of iron-based nanoparticles using oolong tea extract for the degradation of malachite green. *Spectrochim. Acta Mol. Biomol. Spectrosc.* 117, 801–804.
- Huang, X., Muhammad, F., Yu, L., Jiao, B., Shiao, Y., Li, D., 2018. Reduction/immobilization of chromite ore processing residue using composite materials based geopolymer coupled with zero-valent iron. *Ceram. Int.* 44 (3), 3454–3463.
- Huang, X., Zhuang, R., Muhammad, F., Yu, L., Shiao, Y., Li, D., 2017. Solidification/stabilization of chromite ore processing residue using alkali-activated composite cementitious materials. *Chemosphere* 168, 300–308.
- Jagupilla, S.C., Wazne, M., Moon, D.H., 2015. Assessment of ferrous chloride and Portland cement for the remediation of chromite ore processing residue. *Chemosphere* 136, 95–101.
- Jaturapitakkul, C., Tangpagasit, J., Songmue, S., Kiattikomol, K., 2011. Filler effect of fine particle sand on the compressive strength of mortar. *Int. J. Miner. Metall. Mater.* 18 (2), 240–246.
- Juenger, M.C.G., Winnefeld, F., Provis, J.L., Ideker, J.H., 2011. Advances in alternative cementitious binders. *Cement Concr. Res.* 41 (12), 1232–1243.
- Kuang, Y., Wang, Q., Chen, Z., Megharaj, M., Naidu, R., 2013. Heterogeneous Fenton-like oxidation of monochlorobenzene using green synthesis of iron nanoparticles. *J. Colloid Interface Sci.* 410, 67–73.
- Kumar, R., Singh, N., Pandey, S.N., 2015. Potential of green synthesized zero-valent iron nanoparticles for remediation of lead-contaminated water. *Int. J. Environ. Sci. Technol.* 12 (12), 3943–3950.
- Lehoux, A.P., Sanchez-Hachair, A., Lefebvre, G., Carlier, G., Hébrard, C., Lima, A.T., Hofmann, A., 2017. Chromium (VI) retrieval from chromium ore processing residues by electrokinetic treatment. *Water, Air, Soil Pollut.* 228 (9), 378.
- Levankumar, L., Muthukumar, V., Gobinath, M.B., 2009. Batch adsorption and kinetics of chromium (VI) removal from aqueous solutions by *Ocimum americanum* L. seed pods. *J. Hazard Mater.* 161 (2), 709–713.
- Li, J., Chen, Z., Shen, J., Wang, B., Fan, L., 2015. The enhancement effect of pre-reduction using zero-valent iron on the solidification of chromite ore processing residue by blast furnace slag and calcium hydroxide. *Chemosphere* 134, 159–165.
- Madhavi, V., Prasad, T.N.V.K.V., Reddy, A.V.B., Ravindra Reddy, B., Madhavi, G., 2013. Application of phyto-genic zerovalent iron nanoparticles in the adsorption of

- hexavalent chromium. *Spectrochim. Acta Mol. Biomol. Spectrosc.* 116, 17–25.
- Malaviya, P., Singh, A., 2011. Physicochemical technologies for remediation of chromium-containing waters and wastewaters. *Crit. Rev. Environ. Sci. Technol.* 41 (12), 1111–1172.
- Malviya, R., Chaudhary, R., 2006. Factors affecting hazardous waste solidification/stabilization: a review. *J. Hazard Mater.* 137 (1), 267–276.
- Meng, Q., Wu, C., Su, Y., Li, J., Liu, J., Pang, J., 2019. A study of steel wire mesh reinforced high performance geopolymer concrete slabs under blast loading. *J. Clean. Prod.* 210, 1150–1163.
- Mohan Kumar, K., Mandal, B.K., Siva Kumar, K., Sreedhara Reddy, P., Sreedhar, B., 2013. Biobased green method to synthesise palladium and iron nanoparticles using *Terminalia chebula* aqueous extract. *Spectrochim. Acta Mol. Biomol. Spectrosc.* 102, 128–133.
- Muhammad, F., Huang, X., Li, S., Xia, M., Zhang, M., Liu, Q., Shehzad Hassan, M.A., Jiao, B., Yu, L., Li, D., 2018. Strength evaluation by using polycarboxylate superplasticizer and solidification efficiency of Cr⁶⁺, Pb²⁺ and Cd²⁺ in composite based geopolymer. *J. Clean. Prod.* 188, 807–815.
- Mystrioti, C., Xenidis, A., Papassiopi, N., 2014. Application of iron nanoparticles synthesized by green tea for the removal of hexavalent chromium in column tests. *J. Geosci. Environ. Prot.* 2, 28–36.
- Nikolić, V., Komljenović, M., Džunuzović, N., Ivanović, T., Miladinović, Z., 2017. Immobilization of hexavalent chromium by fly ash-based geopolymers. *Compos. B Eng.* 112, 213–223.
- Palomo, A., Palacios, M., 2003. Alkali-activated cementitious materials: alternative matrices for the immobilisation of hazardous wastes: Part II. Stabilisation of chromium and lead. *Cement Concr. Res.* 33 (2), 289–295.
- Qian, G., Cao, Y., Chui, P., Tay, J., 2006. Utilization of MSWI fly ash for stabilization/solidification of industrial waste sludge. *J. Hazard Mater.* 129 (1), 274–281.
- Ranjbar, N., Mehrali, M., Behnia, A., Alengaram, U.J., Jumaat, M.Z., 2014. Compressive strength and microstructural analysis of fly ash/palm oil fuel ash based geopolymer mortar. *Mater. Des.* 59, 532–539.
- Santos, S.A.O., Villaverde, J.J., Freire, C.S.R., Domingues, M.R.M., Neto, C.P., Silvestre, A.J.D., 2012. Phenolic composition and antioxidant activity of *Eucalyptus grandis*, *E. urograndis* (*E. grandis* × *E. urophylla*) and *E. maidenii* bark extracts. *Ind. Crops Prod.* 39, 120–127.
- Shahwan, T., Abu Sirriah, S., Nairat, M., Boyacı, E., Eroğlu, A.E., Scott, T.B., Hallam, K.R., 2011. Green synthesis of iron nanoparticles and their application as a Fenton-like catalyst for the degradation of aqueous cationic and anionic dyes. *Chem. Eng. J.* 172 (1), 258–266.
- Shi, C., Fernández-Jiménez, A., 2006. Stabilization/solidification of hazardous and radioactive wastes with alkali-activated cements. *J. Hazard Mater.* 137 (3), 1656–1663.
- Su, C., Ludwig, R.D., 2005. Treatment of hexavalent chromium in chromite ore processing solid waste using a mixed reductant solution of ferrous sulfate and sodium dithionite. *Environ. Sci. Technol.* 39 (16), 6208–6216.
- Tastan Erdem, O., Edil Tuncer, B., Benson Craig, H., Aydilek Ahmet, H., 2011. Stabilization of organic soils with fly ash. *J. Geotech. Geoenviron. Eng.* 137 (9), 819–833.
- Wang, T., Jin, X., Chen, Z., Megharaj, M., Naidu, R., 2014a. Green synthesis of Fe nanoparticles using eucalyptus leaf extracts for treatment of eutrophic wastewater. *Sci. Total Environ.* 466–467, 210–213.
- Wang, T., Lin, J., Chen, Z., Megharaj, M., Naidu, R., 2014b. Green synthesized iron nanoparticles by green tea and eucalyptus leaves extracts used for removal of nitrate in aqueous solution. *J. Clean. Prod.* 83, 413–419.
- Wang, T., Su, J., Jin, X., Chen, Z., Megharaj, M., Naidu, R., 2013. Functional clay supported bimetallic nZVI/Pd nanoparticles used for removal of methyl orange from aqueous solution. *J. Hazard Mater.* 262, 819–825.
- Wang, Y., Han, F., Mu, J., 2018. Solidification/stabilization mechanism of Pb(II), Cd(II), Mn(II) and Cr(III) in fly ash based geopolymers. *Constr. Build. Mater.* 160, 818–827.
- Xia, M., Muhammad, F., Zeng, L., Li, S., Huang, X., Jiao, B., Shiau, Y., Li, D., 2019. Solidification/stabilization of lead-zinc smelting slag in composite based geopolymer. *J. Clean. Prod.* 209, 1206–1215.
- Xu, W., Li, X., Zhou, Q., Peng, Z., Liu, G., Qi, T., 2011. Remediation of chromite ore processing residue by hydrothermal process with starch. *Process Saf. Environ. Protect.* 89 (3), 179–185.
- Yoon, I.-H., Moon, D.H., Kim, K.-W., Lee, K.-Y., Lee, J.-H., Kim, M.G., 2010. Mechanism for the stabilization/solidification of arsenic-contaminated soils with Portland cement and cement kiln dust. *J. Environ. Manag.* 91 (11), 2322–2328.
- Yu, S., Du, J., Luo, T., Huang, Y., Jing, C., 2012. Evaluation of chromium bioaccessibility in chromite ore processing residue using in vitro gastrointestinal method. *J. Hazard Mater.* 209–210, 250–255.
- Yuan, P., Fan, M., Yang, D., He, H., Liu, D., Yuan, A., Zhu, J., Chen, T., 2009. Montmorillonite-supported magnetite nanoparticles for the removal of hexavalent chromium [Cr(VI)] from aqueous solutions. *J. Hazard Mater.* 166 (2), 821–829.
- Zhang, J., Provis, J.L., Feng, D., van Deventer, J.S.J., 2008. Geopolymers for immobilization of Cr⁶⁺, Cd²⁺, and Pb²⁺. *J. Hazard Mater.* 157 (2), 587–598.
- Zhang, M., Yang, C., Zhao, M., Yang, K., Shen, R., Zheng, Y., 2017. Immobilization potential of Cr(VI) in sodium hydroxide activated slag pastes. *J. Hazard Mater.* 321, 281–289.
- Zhuang, X.Y., Chen, L., Komarneni, S., Zhou, C.H., Tong, D.S., Yang, H.M., Yu, W.H., Wang, H., 2016. Fly ash-based geopolymer: clean production, properties and applications. *J. Clean. Prod.* 125, 253–267.